Higher fidelity benchmarking of the nonlinear Compton and Breit-Wheeler processes in a laser pulse

B. King

b.king@plymouth.ac.uk

UNIVERSITY OF PLYMOUTH

ExHILP 21

13-9-21

T. Blackburn
University of Gothenburg

A. J. Macleod, T. Heinzl
University of Plymouth

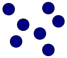

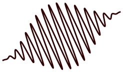

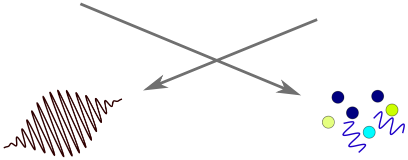

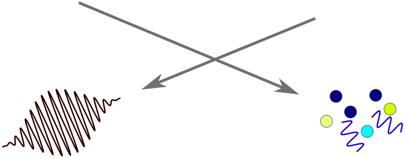

Motivation:

- High-energy experiments, LUXE @ DESY, E320 @ SLAC

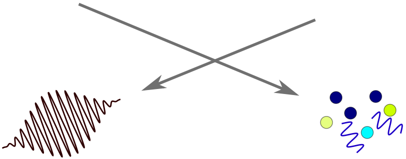

Motivation:

- High-energy experiments, LUXE @ DESY, E320 @ SLAC
- Conventionally-accelerated beams, higher precision measurements

H. Abramowicz et al. arXiv:2102.02032

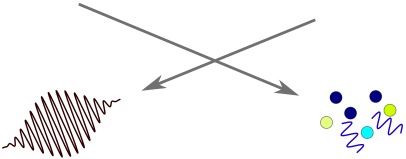

Motivation:

- High-energy experiments, LUXE @ DESY, E320 @ SLAC
- Conventionally-accelerated beams, higher precision measurements

H. Abramowicz et al. arXiv:2102.02032

⇒ See talks by B. Heinemann and N. Tal Hod, Wednesday @ ExHILP

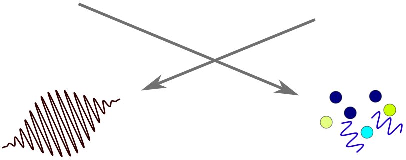

Motivation:

- High-energy experiments, LUXE @ DESY, E320 @ SLAC
- Conventionally-accelerated beams, higher precision measurements

H. Abramowicz et al. arXiv:2102.02032

⇒ See talks by B. Heinemann and N. Tal Hod, Wednesday @ ExHILP

Challenges:

- Laser pulse ("in" state) is an extended (and complicated) object
- Locally Constant Field Approximation (LCFA) inaccurate when $\xi \not\gg 1$.

- QED ‘locally monochromatic’ rates
- Comparison with QED: Nonlinear Compton
  - Photon yield
  - Energy spectrum
  - Energy-angle spectrum
  - Chirped background
  - Focussed background
- (Comparison with QED: Nonlinear Breit-Wheeler)

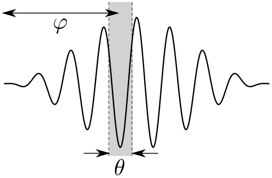

- Kibble mass squared:

$$\mu = m^2 \left[1 + \langle \mathbf{a}^2 \rangle - \langle \mathbf{a} \rangle^2\right]; \qquad \langle f \rangle = \frac{1}{\theta} \int_{\varphi-\theta/2}^{\varphi+\theta/2} f(x) dx$$

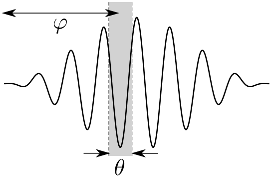

- Kibble mass squared:

$$\mu = m^2 \left[1 + \langle \mathbf{a}^2 \rangle - \langle \mathbf{a} \rangle^2\right]; \qquad \langle f \rangle = \frac{1}{\theta} \int_{\varphi-\theta/2}^{\varphi+\theta/2} f(x) dx$$

e.g. $\mathbf{a} = m\xi \left(\cos\varphi, \sin\varphi, 0\right)$

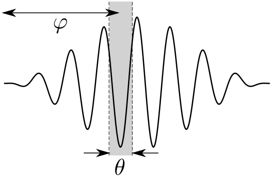

- Kibble mass squared:

$$\mu = m^2 \left[1 + \langle \mathbf{a}^2 \rangle - \langle \mathbf{a} \rangle^2\right]; \qquad \langle f \rangle = \frac{1}{\theta} \int_{\varphi-\theta/2}^{\varphi+\theta/2} f(x) dx$$

e.g. $\mathbf{a} = m\xi\,(\cos\varphi, \sin\varphi, 0)$

$$\mu = m^2 \left[1 + \xi^2 + \frac{2\xi^2(\cos\theta - 1)}{\theta^2}\right]$$

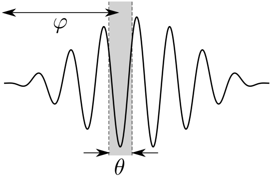

- Kibble mass squared:

$$\mu = m^2\left[1+\langle \mathbf{a}^2\rangle - \langle \mathbf{a}\rangle^2\right]; \qquad \langle f\rangle = \frac{1}{\theta}\int_{\varphi-\theta/2}^{\varphi+\theta/2} f(x)dx$$

e.g. $\mathbf{a} = m\xi\,(\cos\varphi, \sin\varphi, 0)$

$$\mu = m^2\left[1+\xi^2+\frac{2\xi^2(\cos\theta-1)}{\theta^2}\right]$$

$$\mu_{\mathrm{LCFA}} = m^2\left[1+\frac{\xi^2\theta^2}{12}\right]$$

- Plane wave pulse: $\mathbf{a} = \mathbf{e}_x m\xi \, g\left(\frac{\varphi}{\Phi}\right) \cos\varphi.$

- Plane wave pulse: $\mathbf{a} = \mathbf{e}_x m\xi\, g\left(\frac{\varphi}{\Phi}\right)\cos\varphi.$

$$\langle \mathbf{a} \rangle = \mathbf{e}_x \frac{m\xi}{\theta}\left[F\left(\frac{x}{\Phi}\right)\sin x + G\left(\frac{x}{\Phi}\right)\cos x\right]_{\varphi-\theta/2}^{\varphi+\theta/2},$$

$$\begin{aligned} F\left(\frac{x}{\Phi}\right) &= g\left(\frac{x}{\Phi}\right) - \frac{1}{\Phi^2} g''\left(\frac{x}{\Phi}\right) + \ldots \\ G\left(\frac{x}{\Phi}\right) &= \frac{1}{\Phi} g'\left(\frac{x}{\Phi}\right) - \frac{1}{\Phi^3} g'''\left(\frac{x}{\Phi}\right) + \ldots \end{aligned}$$

- Plane wave pulse: $\mathbf{a} = \mathbf{e}_x m\xi\, g\left(\frac{\varphi}{\Phi}\right)\cos\varphi.$

$$\langle \mathbf{a}\rangle = \mathbf{e}_x \frac{m\xi}{\theta}\left[F\left(\frac{x}{\Phi}\right)\sin x + G\left(\frac{x}{\Phi}\right)\cos x\right]_{\varphi-\theta/2}^{\varphi+\theta/2},$$

$$\begin{aligned} F\left(\frac{x}{\Phi}\right) &= g\left(\frac{x}{\Phi}\right) - \frac{1}{\Phi^2}g''\left(\frac{x}{\Phi}\right) + \ldots \\ G\left(\frac{x}{\Phi}\right) &= \frac{1}{\Phi}g'\left(\frac{x}{\Phi}\right) - \frac{1}{\Phi^3}g'''\left(\frac{x}{\Phi}\right) + \ldots \end{aligned}$$

- A ‘locally monochromatic approximation’ results when:
  - Neglect Φ^{-1} factors and higher
  - Taylor expand in θ and keep lowest order terms

$$\Rightarrow \langle \mathbf{a}\rangle \approx \mathbf{e}_x \frac{m\xi}{\theta} g\left(\frac{\varphi}{\Phi}\right)\sin\varphi = g\left(\frac{\varphi}{\Phi}\right)\langle \mathbf{a}_{\mathrm{mono}}\rangle$$

$$\mathsf{P}_{\mathsf{LMA}} = \int d\tau \; \mathsf{R}_{\mathsf{mono}}\left[\xi\, g\left(\frac{\tau}{T}\right)\right]$$

$$\mathsf{P}_{\mathsf{LMA}} = \int d\tau \; \mathsf{R}_{\mathsf{mono}}\left[\xi \, g\left(\frac{\tau}{T}\right)\right]$$

$$\text{c.f.} \quad \mathsf{P}_{\mathsf{LCFA}} = \int d\tau \; \mathsf{R}_{\mathsf{ccf}}\left[\xi'(\tau)\right]$$

$$\mathrm{P}_{\mathrm{LMA}} = \int d\tau\, \mathrm{R}_{\mathrm{mono}}\left[\xi\, g\left(\frac{\tau}{T}\right)\right]$$

$$\text{c.f.}\quad \mathrm{P}_{\mathrm{LCFA}} = \int d\tau\, \mathrm{R}_{\mathrm{ccf}}\left[\xi'(\tau)\right]$$

- LCFA depends on the instantaneous momentum:

$$\mathrm{R}_{\mathrm{LCFA}} = \mathrm{R}_{\mathrm{LCFA}}(\pi); \qquad \pi = p - a + \varkappa\,\frac{2p\cdot a - a^2}{2\,\varkappa\cdot p}$$

$$\mathsf{P}_{\mathsf{LMA}} = \int d\tau\, \mathsf{R}_{\mathsf{mono}}\left[\xi\, g\left(\frac{\tau}{T}\right)\right]$$

$$\text{c.f.} \quad \mathsf{P}_{\mathsf{LCFA}} = \int d\tau\, \mathsf{R}_{\mathsf{ccf}}\left[\xi'(\tau)\right]$$

- LCFA depends on the instantaneous momentum:

$$\mathsf{R}_{\mathsf{LCFA}} = \mathsf{R}_{\mathsf{LCFA}}(\pi); \qquad \pi = p - a + \varkappa\,\frac{2p\cdot a - a^2}{2\,\varkappa\cdot p}$$

- LMA depends on the cycle-average momentum:

$$\mathsf{R}_{\mathsf{LMA}} = \sum_n \mathsf{R}^{(n)}_{\mathsf{LMA}}(a^2_{\mathrm{rms}}); \qquad a^2_{\mathrm{rms}} = \frac{\langle\pi\rangle^2_{\varphi}}{m^2} - 1$$

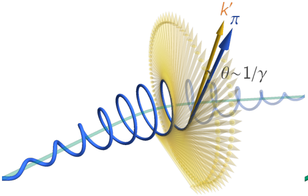

k'
π
$\theta \sim 1/\gamma$

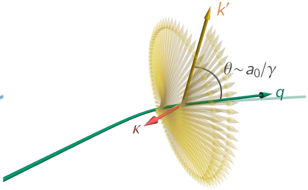

k'
$\theta \sim a_0/\gamma$
q
κ

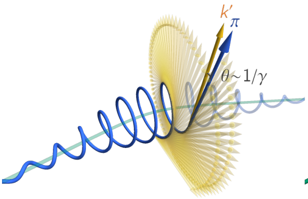

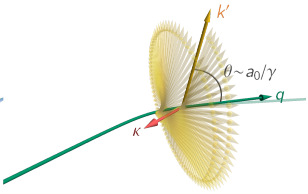

	LCFA	LMA
rate derived for	constant, crossed field	monochromatic plane wave (*fast quiver motion here*)
and controlled by	instantaneous momentum π^μ via quantum parameter χ_e	quasimomentum $q^\mu = \langle \pi^\mu \rangle_\varphi$ via a_{rms} and η
equation of motion	Lorentz force: $\frac{d\pi_\mu}{d\tau} = -\frac{eF_{\mu\nu}\pi^\nu}{m}$ (*fast quiver motion here*)	ponderomotive force: $\frac{d\vec{q}}{dt} = -\frac{m^2}{2q^0}\frac{\partial a_{\text{rms}}^2}{\partial \vec{r}}$

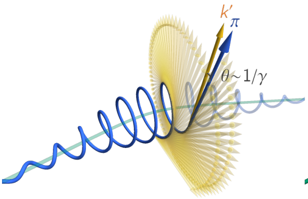

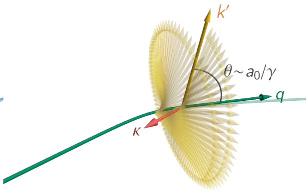

	LCFA	LMA
rate derived for	constant, crossed field	monochromatic plane wave (*fast quiver motion here*)
and controlled by	instantaneous momentum π^{μ} via quantum parameter χ_e	quasimomentum $q^{\mu} = \langle \pi^{\mu} \rangle_{\varphi}$ via a_{rms} and η
equation of motion	Lorentz force: $\frac{d\pi_{\mu}}{d\tau} = -\frac{eF_{\mu\nu}\pi^{\nu}}{m}$ (*fast quiver motion here*)	ponderomotive force: $\frac{d\vec{q}}{dt} = -\frac{m^2}{2q^0}\frac{\partial a^2_{\text{rms}}}{\partial \vec{r}}$

⇒ See tutorial talk by T. Blackburn, Tuesday @ ExHILP

- Ptarmigan, https://github.com/tgblackburn/ptarmigan

- Ptarmigan, https://github.com/tgblackburn/ptarmigan
- E144 locally monochromatic rate

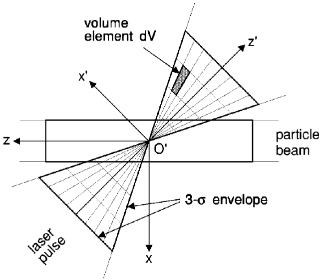

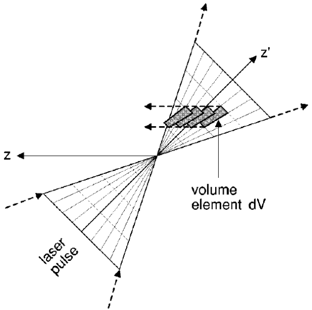

C. Bamber et al., Phys. Rev. D **60**, 092004 (1999)

- Ptarmigan, https://github.com/tgblackburn/ptarmigan
- E144 locally monochromatic rate

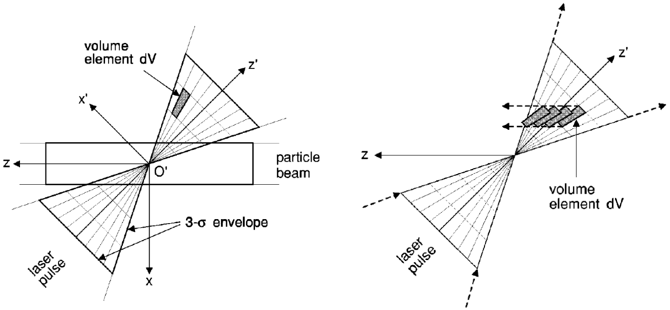

C. Bamber et al., Phys. Rev. D **60**, 092004 (1999)

- CAIN, P. Chen et al., Nucl. Instrum. Methods Phys. Res. A, 355, 107, (1995)
- IPStrong, A. Hartin, Int. J. Mod. Phys. A, 33, 1830011 (2018)

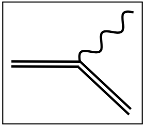

Nonlinear Compton Scattering

‘QED result’:	‘LMA simulation result’:
QED	QED
↓	↓
‘Plane-wave’ QED	‘Plane-wave’ QED
	↓
	LMA

'QED result':	'LMA simulation result':
QED	QED
↓	↓
'Plane-wave' QED	'Plane-wave' QED
	↓
	LMA

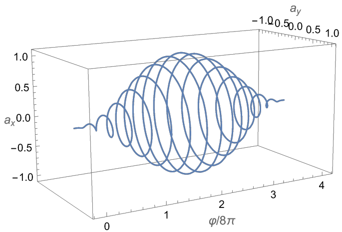

$$\mathbf{a} = e\mathbf{A} = m\xi \sin^2\left(\frac{\varphi}{2N}\right)\{\cos\varphi, \sin\varphi, 0\}$$

$$\frac{\text{'QED result':}}{\text{QED}} \quad \downarrow \quad \text{'Plane-wave' QED}$$

$$\frac{\text{'LMA simulation result':}}{\text{QED}} \quad \downarrow \quad \text{'Plane-wave' QED} \quad \downarrow \quad \text{LMA}$$

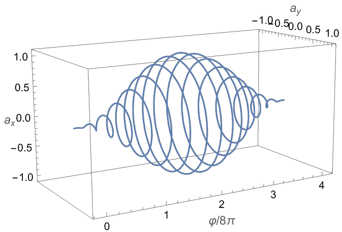

$$\mathbf{a} = e\mathbf{A} = m\xi \sin^2\left(\frac{\varphi}{2N}\right)\{\cos\varphi, \sin\varphi, 0\}$$

- ξ, 'classical nonlinearity parameter'
- $\eta = \varkappa \cdot p/m^2$, 'energy parameter' $\quad (\chi = \xi\eta)$
- $\eta = 0.2$ ($\sim 17\,\mathrm{GeV}$ for head-on collision with $1.55\,\mathrm{eV}$ laser photons).
- N number of laser cycles.

$\eta = 0.2, \quad N = 16$

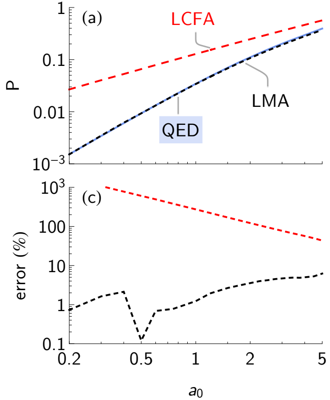

T. G. Blackburn, A. J. MacLeod, BK, NJP **23**, 085008 (2021)

- Error approximated by relative difference of LMA and QED results

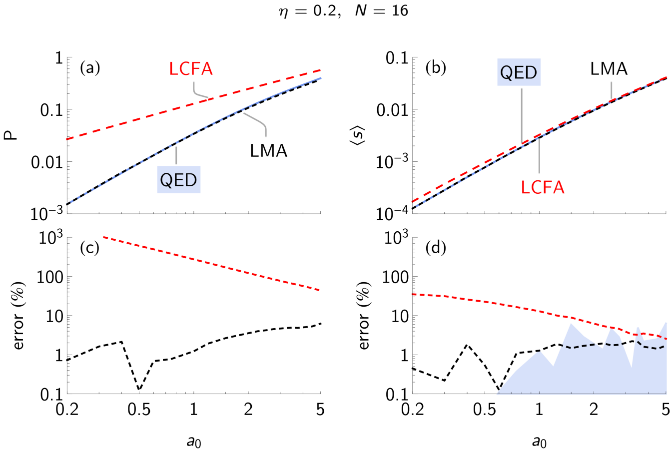

T. G. Blackburn, A. J. MacLeod, BK, NJP **23**, 085008 (2021)

- Error approximated by relative difference of LMA and QED results

$\eta = 0.2$

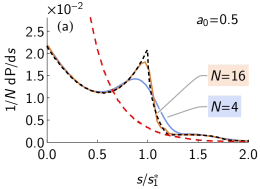

T. G. Blackburn, A. J. MacLeod, BK, NJP **23**, 085008 (2021)

- More accurate as N increased

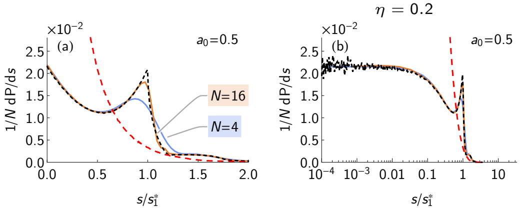

T. G. Blackburn, A. J. MacLeod, BK, NJP **23**, 085008 (2021)

- More accurate as N increased
- Ptarmigan LMA acquires correct IR limit

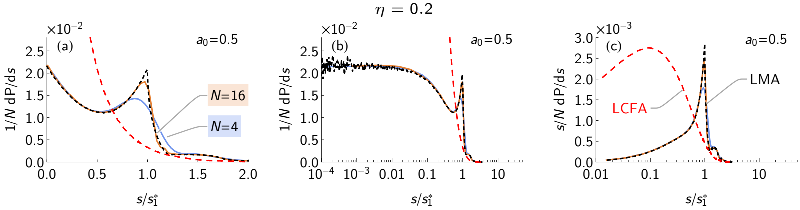

T. G. Blackburn, A. J. MacLeod, BK, NJP **23**, 085008 (2021)

- More accurate as N increased
- Ptarmigan LMA acquires correct IR limit

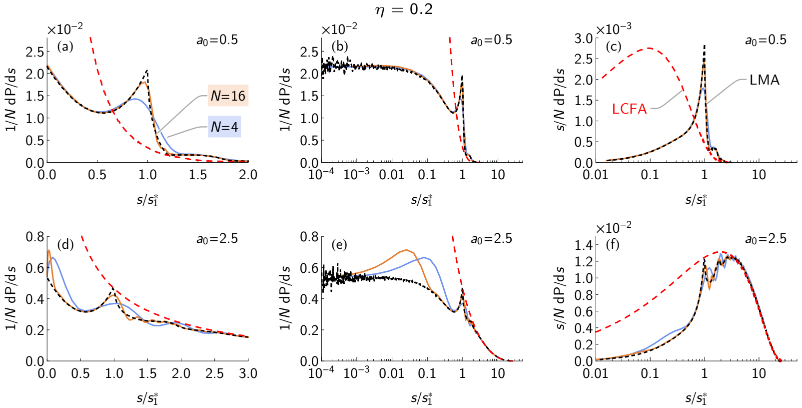

T. G. Blackburn, A. J. MacLeod, BK, NJP **23**, 085008 (2021)

- More accurate as N increased
- Ptarmigan LMA acquires correct IR limit
- Misses mid-IR pulse envelope peaks

BK, PRD 103 (3), 036018 (2021)

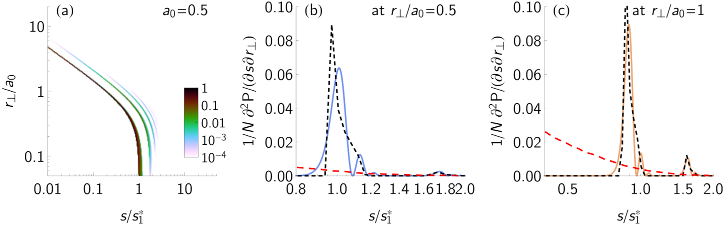

T. G. Blackburn, A. J. MacLeod, BK, NJP **23**, 085008 (2021)

- Angular harmonic position and integral captured by Ptarmigan

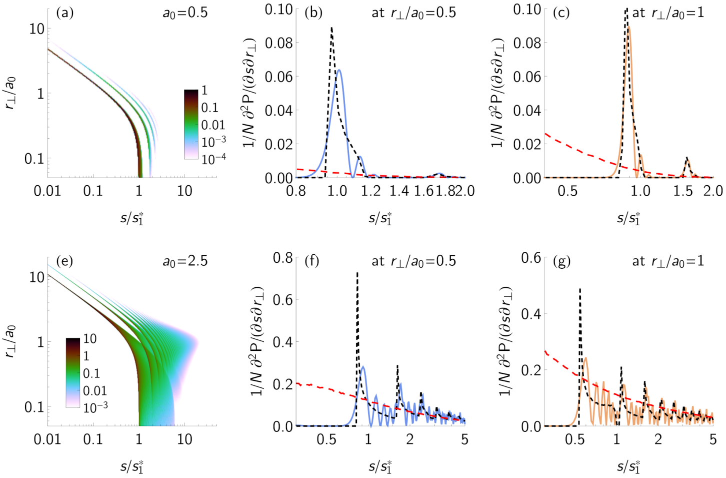

T. G. Blackburn, A. J. MacLeod, BK, NJP **23**, 085008 (2021)

- Angular harmonic position and integral captured by Ptarmigan
- Subharmonics averaged through

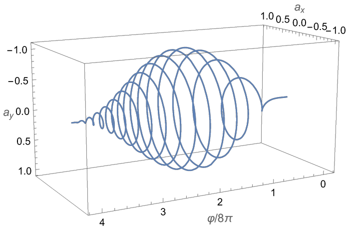

$$\begin{aligned} a &= m\xi \sin^2\left(\frac{\varphi}{2N}\right)\{\cos b(\varphi), \sin b(\varphi), 0\} \\ b(\varphi) &= \varphi + c(\varphi - \pi N)^2 \\ b'(\varphi) &= 1 + 2c(\varphi - \pi N) \end{aligned}$$

- Chirp: spacetime-dependent wavevector

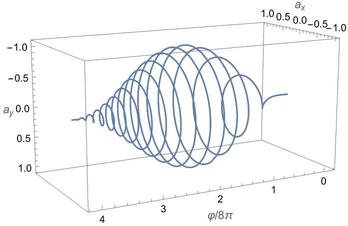

$$a = m\xi \sin^2\left(\frac{\varphi}{2N}\right)\{\cos b(\varphi), \sin b(\varphi), 0\}$$

$$b(\varphi) = \varphi + c(\varphi - \pi N)^2$$

$$b'(\varphi) = 1 + 2c(\varphi - \pi N)$$

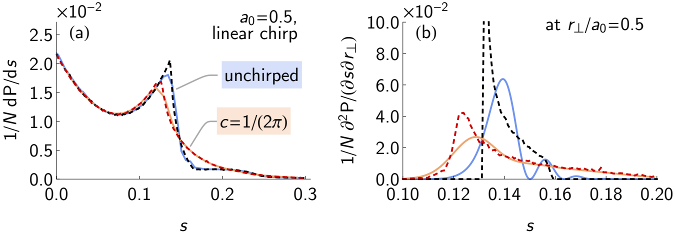

T. G. Blackburn, A. J. MacLeod, BK, NJP **23**, 085008 (2021)

- Chirp: spacetime-dependent wavevector
- Ptarmigan reproduces: softening of Compton edge, smearing of angular spectrum


4 w₀
e⁻ disc
laser

$$P^{QED}_{3D} \approx \int d^2\mathbf{x}^{\perp}\, \rho(\mathbf{x}^{\perp}) P^{QED}_{PW}\left[\mathbf{a}(\mathbf{x}^{\perp})\right]$$

A. Di Piazza, Phys. Rev. Lett. **113**, 040402 (2014)

$$\mathrm{P}^{\mathrm{QED}}_{3D} \approx \int d^2\mathbf{x}^{\perp}\, \rho(\mathbf{x}^{\perp}) \mathrm{P}^{\mathrm{QED}}_{\mathrm{PW}}\left[\mathbf{a}(\mathbf{x}^{\perp})\right]$$

A. Di Piazza, Phys. Rev. Lett. **113**, 040402 (2014)

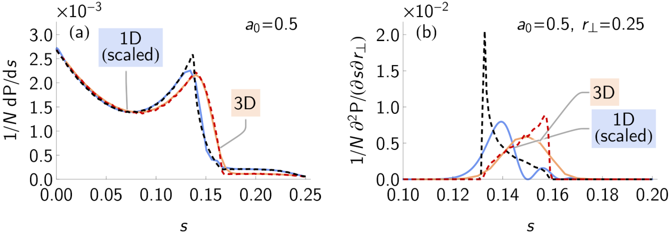

T. G. Blackburn, A. J. MacLeod, BK, NJP **23**, 085008 (2021)

- ‘Smearing’ of Compton edge due to range of impact parameters.

$$\mathrm{P}^{\mathrm{QED}}_{3D} \approx \int d^2\mathbf{x}^{\perp}\,\rho(\mathbf{x}^{\perp})\mathrm{P}^{\mathrm{QED}}_{\mathrm{PW}}\left[\mathbf{a}(\mathbf{x}^{\perp})\right]$$

A. Di Piazza, Phys. Rev. Lett. **113**, 040402 (2014)

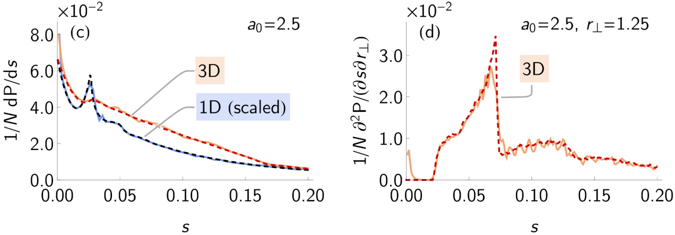

T. G. Blackburn, A. J. MacLeod, BK, NJP **23**, 085008 (2021)

- Second 'edge' at electron disc edge impact parameter.

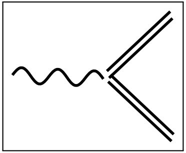

Nonlinear Breit-Wheeler pair creation

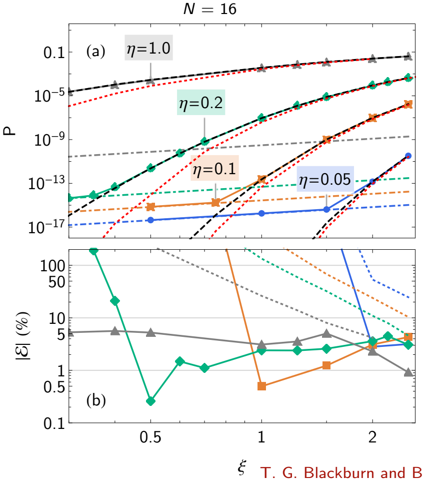

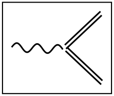

T. G. Blackburn and BK, 2108.10883 [hep-ph] (2021)

NBW: Pair Yield

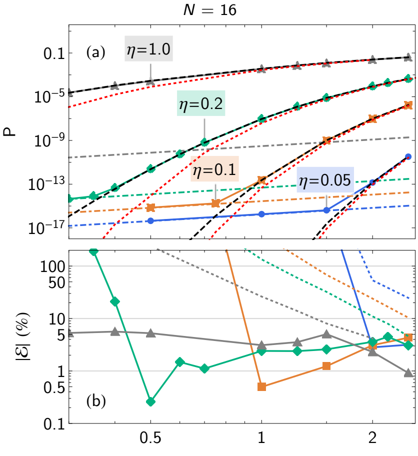

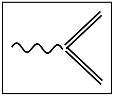

T. G. Blackburn and BK, 2108.10883 [hep-ph] (2021)

- Harmonic threshold $n_* \gg 1$, but LCFA inaccurate if $\xi \not\gg 1$

NBW: Pair Yield

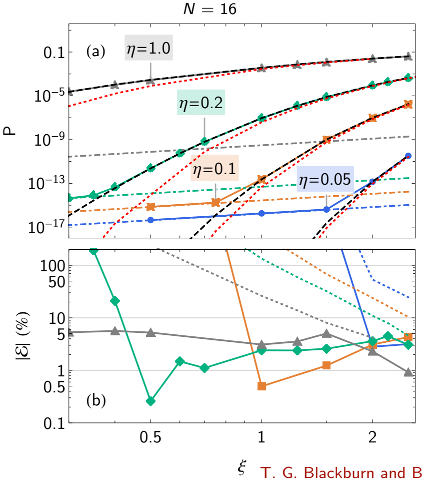

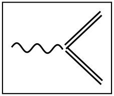

T. G. Blackburn and BK, 2108.10883 [hep-ph] (2021)

- Harmonic threshold $n_* \gg 1$, but LCFA inaccurate if $\xi \not\gg 1$
- For small enough ξ, perturbative contribution from envelope dominates

T. Heinzl, A. Ilderton, M. Marklund, PLB **692**, 250–256 (2010)
T. Nousch, D. Seipt, B. Kämpfer and A. I. Titov, PLB **715**, 246–250 (2012)

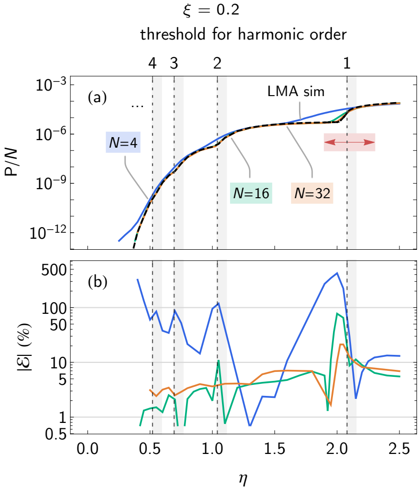

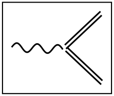

T. G. Blackburn and BK, 2108.10883 [hep-ph] (2021)

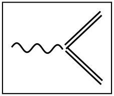

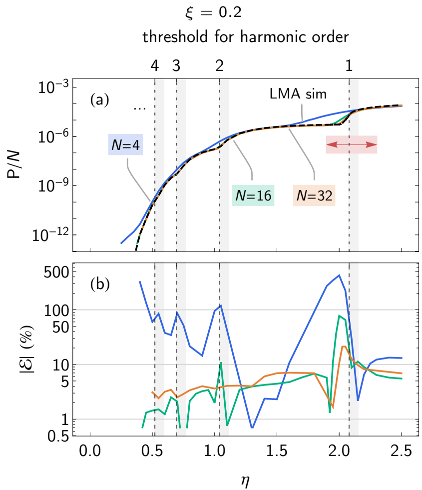

T. G. Blackburn and BK, 2108.10883 [hep-ph] (2021)

Simulation error decreases with N, but increases at channel openings

S. Tang and BK, 2109.00555 (2021)

$\eta = 0.2, \quad N = 16$

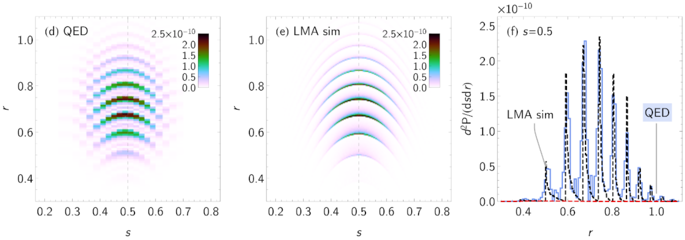

T. G. Blackburn and BK, 2108.10883 [hep-ph] (2021)

$\eta = 0.2, \quad N = 16$

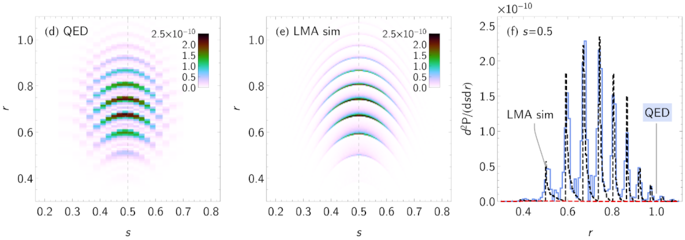

T. G. Blackburn and BK, 2108.10883 [hep-ph] (2021)

- Angular harmonic position and integral captured by simulation

$\eta = 0.2, \quad N = 16$

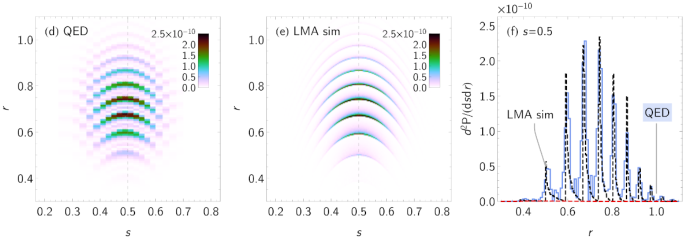

T. G. Blackburn and BK, 2108.10883 [hep-ph] (2021)

- Angular harmonic position and integral captured by simulation
- Subharmonics averaged through

$\eta = 0.2, \quad N = 16$

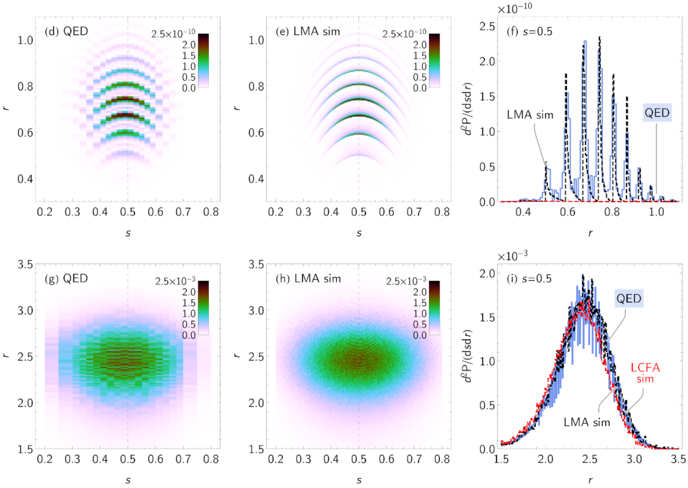

T. G. Blackburn and BK, 2108.10883 [hep-ph] (2021)

- Angular harmonic position and integral captured by simulation
- Subharmonics averaged through

$$P^{\text{QED}}_{3D} \approx \int d^2\mathbf{x}^{\perp}\, \rho(\mathbf{x}^{\perp}) P^{\text{QED}}_{\text{PW}}\left[\mathbf{a}(\mathbf{x}^{\perp})\right]$$

$\eta = 0.2, \quad N = 16$

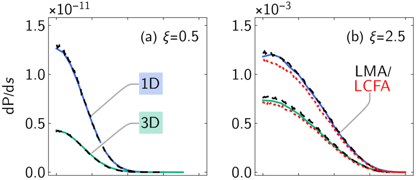

$$P_{3D}^{\text{QED}} \approx \int d^2\mathbf{x}^\perp \, \rho(\mathbf{x}^\perp) P_{\text{PW}}^{\text{QED}} \left[\mathbf{a}(\mathbf{x}^\perp) \right]$$

$\eta = 0.2, \quad N = 16$

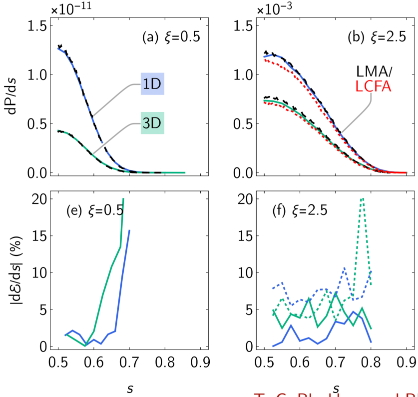

T. G. Blackburn and BK, 2108.10883 [hep-ph] (2021)

$$P^{\text{QED}}_{3D} \approx \int d^2\mathbf{x}^{\perp}\, \rho(\mathbf{x}^{\perp}) P^{\text{QED}}_{\text{PW}}\left[\mathbf{a}(\mathbf{x}^{\perp})\right]$$

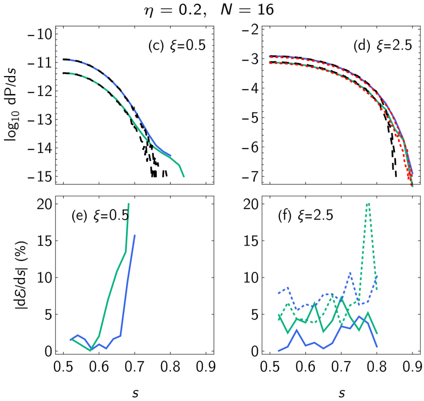

T. G. Blackburn and BK, 2108.10883 [hep-ph] (2021)

- Ptarmigan uses ponderomotive scattering + LMA event generator to calculate strong-field QED effects.

- Ptarmigan uses ponderomotive scattering + LMA event generator to calculate strong-field QED effects.
- Benchmarking with plane-wave QED result, 'theory error' $\sim O(1/N)$.

- Ptarmigan uses ponderomotive scattering + LMA event generator to calculate strong-field QED effects.
- Benchmarking with plane-wave QED result, ‘theory error’ $\sim O(1/N)$.
- LMA error can increase around channel openings, and misses pulse envelope effects.

- Ptarmigan uses ponderomotive scattering + LMA event generator to calculate strong-field QED effects.
- Benchmarking with plane-wave QED result, 'theory error' $\sim O(1/N)$.
- LMA error can increase around channel openings, and misses pulse envelope effects.
- Future work includes: linearly polarised background, particle polarisation.

- Ptarmigan uses ponderomotive scattering + LMA event generator to calculate strong-field QED effects.
- Benchmarking with plane-wave QED result, 'theory error' $\sim O(1/N)$.
- LMA error can increase around channel openings, and misses pulse envelope effects.
- Future work includes: linearly polarised background, particle polarisation.

- LMA(simulation) v QED (Compton): T. G. Blackburn, A. J. MacLeod, BK, NJP **23**, 085008 (2021)
- LMA(simulation) v QED (Pairs): T. G. Blackburn and BK, 2108.10883 [hep-ph] (2021)
- LMA: T. Heinzl, BK, A. J. Macleod, PRA **102** (6), 063110 (2020)
- QED envelope effects beyond LMA (Compton): BK, PRD 103 (3), 036018 (2021)
- QED envelope effects beyond LMA (Pairs): S. Tang and BK, arXiv:2109.00555 (2021)

Ptarmigan: https://github.com/tgblackburn/ptarmigan